CONEM 2016
CONGRESSO NACIONAL DE ENGENHARIA MECÂNICA
21 - 25 AGOSTO DE 2016
FORTALEZA - CEARÁ

CON-2016-1601 – SOLID STATE REACTIONS AND THERMODYNAMICS OF STRONTIUM ALUMINATES VIA ($SrO—Al_2O_3$).B_2O_3 FOR LUMINESCENT NANO PHOSPHORS

Nadia Khaled Zurba, f2698@ua.pt[1,2]
José Maria da Fonte Ferreira, jmf@ua.pt[2]

[1]Federal University of Ceará, Centre of Technology (CT), 60.020-181, Fortaleza, Ceará, Brazil,
[2]University of Aveiro, Aveiro Institute of Materials, Centre for Research in Ceramic and Composite Materials (CICECO), 3810-193, Aveiro, Portugal

Abstract: *Strontium aluminate materials were prepared by solid-state reactions. Some independent factors of the host lattices crystallization, such as thermo chemical performance of the reagents and the effects of boron flux addition are reported. A number of balanced compositions on the ($SrO–Al_2O_3$).B_2O_3 system using a phase diagram were studied. The elucidation of the thermodynamic features of the crystallization was commenced with measurements of XRD, DTA, TG, SEM and HR-TEM analysis.*

Key-words: *solid-state reactions, thermodynamic, enthalpy, strontium aluminate, host lattice, crystallization.*

1. INTRODUCTION

Strontium aluminate lanthanide co-doped ($SrAl_2O_4$:Ln) is a type of luminescent material about 10 times brighter, 10 times longer glowing, and 10 times more expensive than its predecessor copper-activated zinc sulphide (ZnS:Cu) [1]. Strontium aluminate phosphors produce yellow-green, blue-green and blue hues, for the excitation wavelengths from 200 to 450 nm, with wavelength emission at ≈520 nm, blue-green at ≈505 nm, and blue at ≈490 nm, depending of the lanthanide co-doping. Note that "*phosphor*" is a term herein used to designate a lighting material, and does not refer to the chemical element P. This word *phosphor* was invented in the 17th century from a sintered stone that emitted red light in the dark after exposure to sunlight, called "*Bolognian stone*" (actually known as being BaS) in the pigment industry [1f].

Crystalline strontium aluminate compounds of the system S_aA_b (where *a* is the molar ratio of SrO, and *b* is the molar ratio of Al_2O_3), such as $SrAl_2O_4$ (SA), $SrAl_4O_7$ (SA_2), $SrAl_{12}O_{19}$ (SA_6), $Sr_2Al_6O_{11}$ (S_2A_3), $Sr_3Al_2O_6$ (S_3A), $Sr_4Al_{14}O_{25}$ (S_4A_7), are functional materials for persistent luminescence when doped with rare-earth metals. In this family, the $SrAl_2O_4$ is extensively mentioned in the literature as the most efficient host lattice phosphor [2-3].

In the monoclinic α-$SrAl_2O_4$ phase, there are two interstitial sites for cations to occupy, i.e. Sr^{1+} and Sr^{2+}. These sites provide different spatial symmetry and orientation direction that result in emission shifts of Eu-doped phosphors [4]. The $SrAl_2O_4$ has a α-monoclinic structure constructed by corner-sharing [AlO_4]. The charge deficiency introduced by the occupancy of Al^{3+} ions in these tetrahedral is compensated by the incorporation of Sr^{2+} ions within the interstitial sites [5-6]. Lanthanides with compatible ionic ratio might be added as co-dopant luminescent centres. The metastable phase is obtained via an endothermic process at temperatures of about 923 K (ΔH=3.2 kJ/mol) [7-8] presenting β-hexagonal tridymite-type structure [9].

The crystalline structure of luminescent materials that accepts a substitutional lanthanide element in ionic vacancies is called host lattice. The chemical formula for luminescence is expressed as H:A, S, where H is the host lattice material (or matrix, M), A is an activator of luminescence, and S is a sensitizer of the energy transfer mechanism. A special criterion of order between sensitizers and activators (Fig. 1) was arbitrated for $SrAl_2O_4$:Ce^{3+}, Dy^{3+}, Eu^{2+} nanotubes, naowires and core-shells owing the relative quantity of cerium (III) as the main activator doping the strontium aluminate host lattice [10]. From the cationic point of view, the strontium ions in the positions of aluminium are unfavourable to occur.

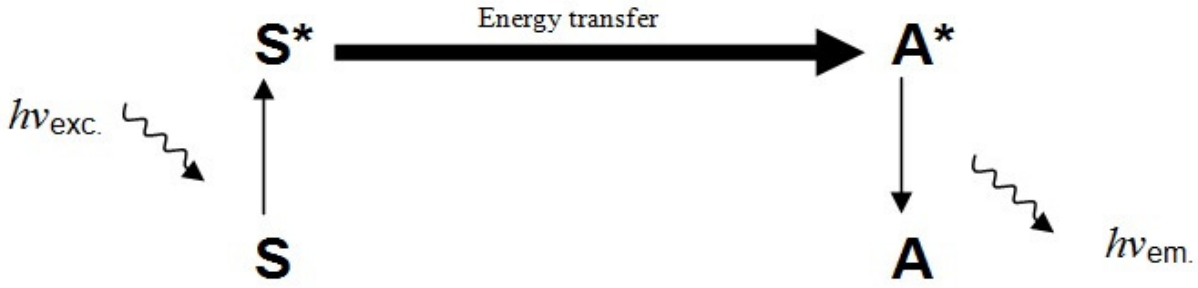

Figure 1. Energy transfer mechanism between sensitizer and activator.

Solid-state reaction is a satisfactory route for the synthesis of co-doped strontium aluminates for large scale applications in luminescence [11], requiring temperatures usually above 1373 K. Recently, the solid-state reaction between $SrCO_3$ and Al_2O_3 has been studied comprising the temperature dependent formation of $SrAl_2O_4$ [9b]. The strontium aluminates are established compounds in the $SrO–Al_2O_3$ system, which crystalline phases formation depend of the starting components, such as the concentration of a catalytic reagent B_2O_3 [12]. The B-doping in tridymite-like structure of $SrAl_2O_4$ drastically reduces the synthesis temperature [13]. A micrometer particle size and coexistence of crystalline phases were generally obtained [13-18]. However, many uncertainties still remain, especially concerning the melting points of many compounds, or more basically the existence of some compounds [4],[11] and [13]. Note that the $SrO—Al_2O_3$ phase diagram [14] does not contain all crystalline compounds (Fig. 2).

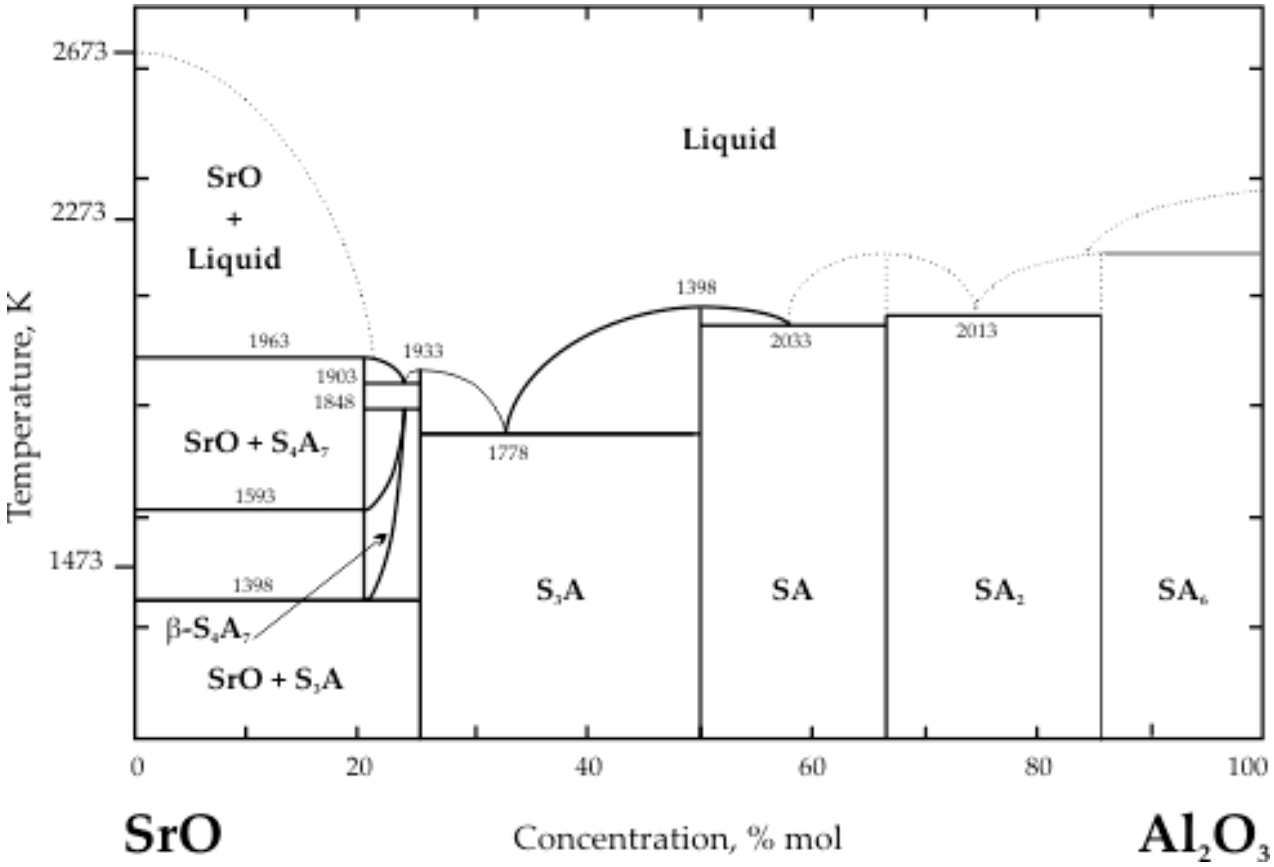

Figure 2. Kelvin temperature conversion of the $SrO—Al_2O_3$ phase diagram [14].

In this article, the synthesis of $SrAl_2O_4$ host lattice crystallization and the formations of strontium aluminates compounds were investigated by the traditional solid state method under a catalyst boric acid addition. Some independent factors of the host lattices crystallization, such as thermo chemical performance of the reagents and the effects of boron flux addition are reported. A number of balanced compositions on the $(SrO–Al_2O_3).B_2O_3$ system using a phase diagram were studied. The elucidation of the thermodynamic features of the crystallization was commenced with measurements of XRD, DTA, TG, SEM and HR-TEM analysis.

2. EXPERIMENTAL

$SrCO_3$ (Aldrich; 99%, orthorhombic) and α-Al_2O_3 (Alcoa), were used as received (Fig. 3). Boric acid, H_3BO_3 (Aldrich, 99.99%), was added in convenient quantity as a fluxing agent to the mixture. Powder materials present particles size distributions from 0.5 to 2.3 μm ($SrCO_3$) and from 0.4 to 3.5 μm (Al_2O_3), measured by Coulter, LS Fraunhofer PIDS. Stoichiometric mixtures, 1:1 molar ratio of $SrCO_3$ and α-Al_2O_3, adding catalyst concentrations of 0.5 mol% (B1) and 1.0 mol% (B2) H_3BO_3 were investigated. The dried (323 K, 3 h) powders mixtures were planetary ball-milled. The as obtained powder mixtures were compacted (200 MPa) into cylindrical pellets, which were heat treated in alumina crucibles under air atmosphere at 1473 K and 1573 K, for 3 and 10 h. The annealed samples were grinded/deagglomerated using an agate mortar for characterization.

Powder microstructure and elemental composition of all samples were observed via scanning electron microscopy (SEM) coupled to energy dispersive X-ray (EDX) spectrometer in a SU-70, and by high-resolution transmission electron microscopy (HR-TEM) in HITACHI-9000 microscopes at University of Aveiro, respectively. For TEM and electron diffraction, powders were ultrasonically dispersed in an ethanol suspension and immersed into copper grids. Crystallizations were characterized by X-ray diffraction (XRD) in a Rigaku Geigerflex D/Mac, C Series diffractometer was used with Cu $K\alpha$ radiation (λ=1.5406 Å) produced at 30 kV and 25 mA scanned the diffraction angles (2θ) between 20º and 70º with a step size of 0.02º 2θ per second. The positions of the characteristic peaks were characterized supported from the indexed cards JCPDS Powder Diffraction Files (PDF) of the International Centre for Diffraction Data (ICDD). The thermo gravimetric (TG) and differential thermal (DTA) analyses of starting compositions and host lattices samples were measured using a TG-DTA Setaram Labsys analyzer in *Argon* atmosphere. The thermodynamic activities on the SrO—Al_2O_3 system within the temperature range of 1473-1573 K were determined using the FactSage 5.5 software in Integrated Thermodynamic Databank System (ITDS).

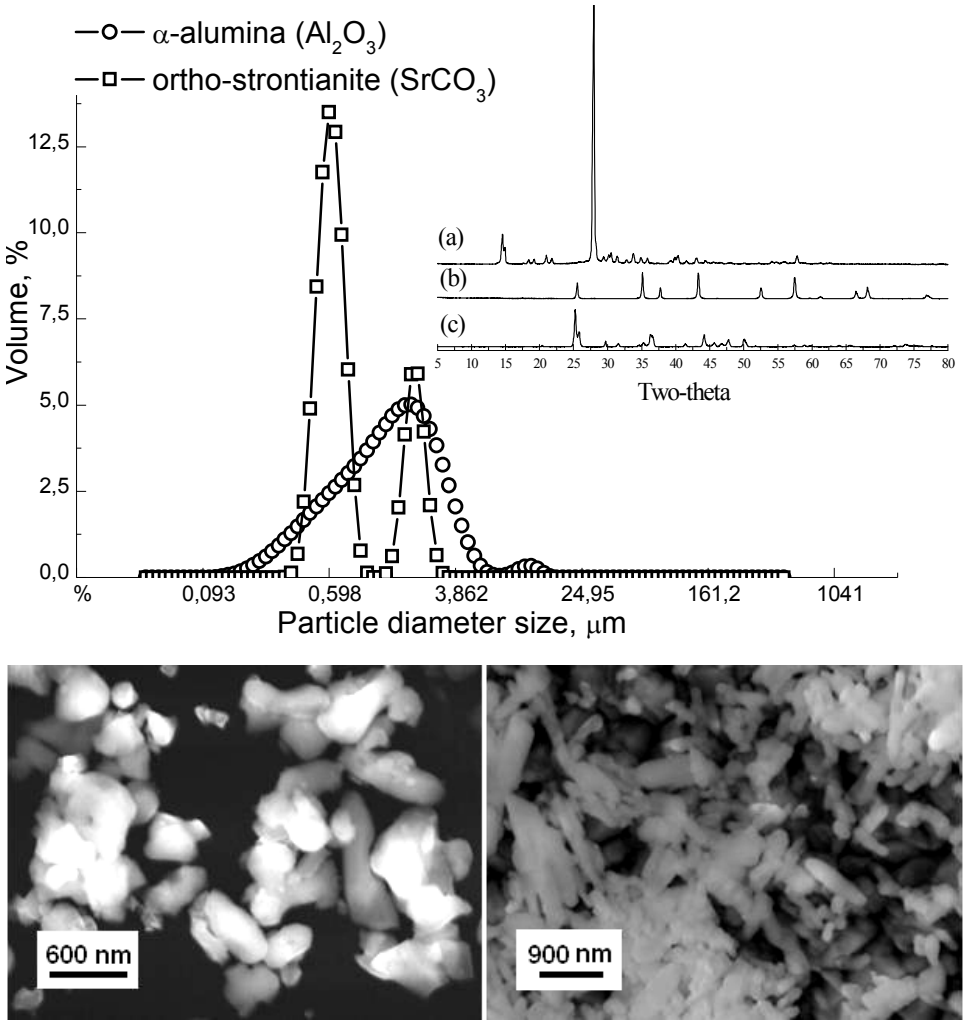

Figure 3. Particles size distributions of $SrCO_3$ and α-Al_2O_3 powders. In detail: X-ray patterns of a) H_3BO_3, b) α-Al_2O_3 and c) ortho-$SrCO_3$. SEM images of powders d) α-Al_2O_3 and e) $SrCO_3$ reagents.

3. RESULTS

3.1. Solid-state reactions and thermodynamics

The solid-state chemical reactions between $SrCO_3$ and Al_2O_3 reagents to form $SrAl_2O_4$ (SA) are described by Eq. (1), (2) and (3).

$$SrCO_{3\,(s)} + Al_2O_{3\,(s)} \xrightarrow{\Delta} SrAl_2O_{4\,(s)} + CO_{2\,(g)} \quad (1)$$

$$SrCO_{3\,(s)} \xrightarrow{\Delta} SrO_{\,(s)} + CO_{2\,(g)} \quad (2)$$

$$SrO_{\,(s)} + Al_2O_{3\,(s)} \xrightarrow{\Delta} SrAl_2O_{4\,(s)} \quad (3)$$

The weight-loss due to thermal decomposition of $SrCO_3$ with release of CO_2 is an essential step to get free SrO to react with Al_2O_3. Considering one mole of $SrCO_3$ (147.63 g), the reaction products after complete thermal decomposition will be one mole of SrO (103.63 g) and one mole of CO_2 (44 g) that is released to the atmosphere (Eq. 2). So, Δm_{SrCO3} (%) = (44/147.63)*100 = 29.8%. This theoretical value of the strontianite weight-loss is coherent with the TG curve obtained during the experimental $SrCO_3$ decomposition process indicated on the thermogram (Δm_{SrCO3}), Fig. 4.

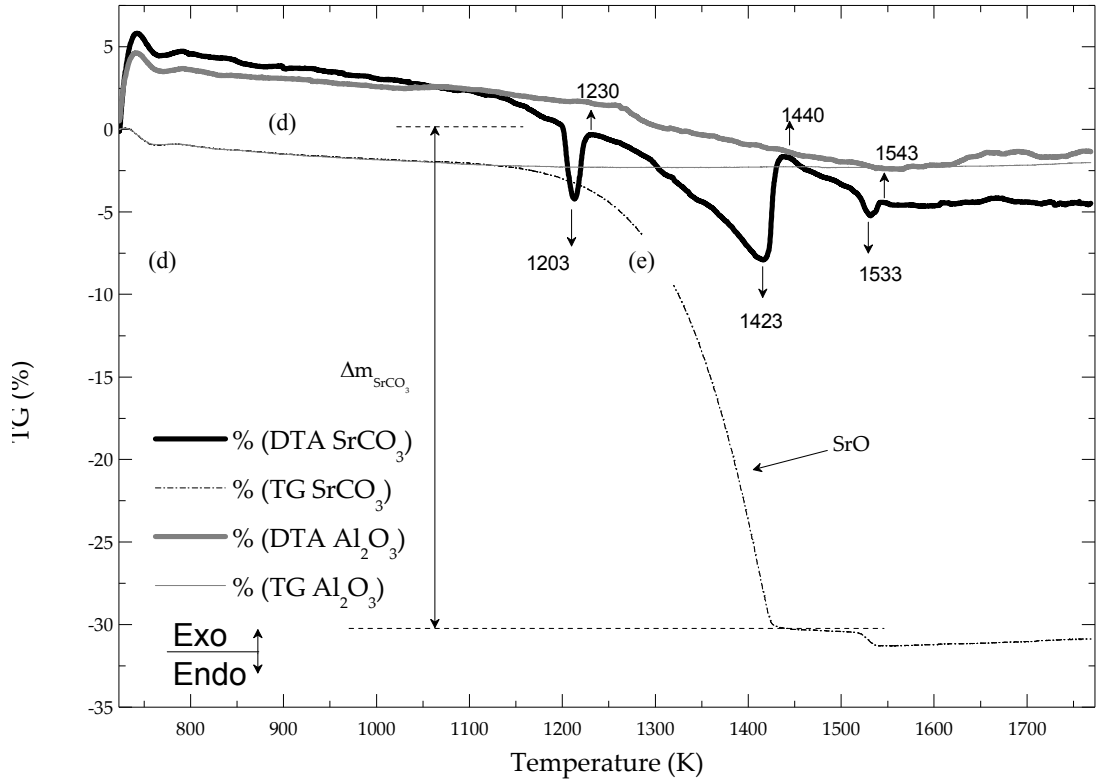

Figure 4. DTA and TG in *Argon* atmosphere at temperatures still 1773 K. Thermograms of separated $SrCO_3$ and Al_2O_3 reagents.

Furthermore, the DTA of $SrCO_3$ from Fig. 4 revealed the follow features, as described.

- **Endothermic peak with a maximum at 1203 K**: attributed to the phase transformation from orthorhombic to hexagonal structure of $SrCO_3$. This polymorphic transformation of $SrCO_3$ structure occurs by the rotational disorder transition of the anion group at a certain temperature, in agreement value reported in literature [15-16]. The phase transformation results in an increase of crystal symmetry and volumetric expansion [7];
- **Endothermic peak with a maximum at 1423 K**: attributed to thermal decomposition of $SrCO_3$ with the release of —CO_2 (g).
- **Exothermic peak centred at 1440 K**: due to the crystallization of SrO.
- **Endothermic peak centred at 1533 K**: probably due to any remaining decarbonisation, since it is concomitant with a small weight loss.

The thermal analysis of $SrCO_3$—Al_2O_3 mixture (50% molar ratio) is presented in Fig. 5. It can be seen that the powders mixture underwent thermal effects similar to those observed for $SrCO_3$ component alone, which tended to appear at somewhat lower temperatures, suggesting that the chemical reaction in the $SrCO_3$—Al_2O_3 system is partially preceded by the decomposition of $SrCO_3$. The DTA curve exhibits the following characteristics, as described.

- **Endothermic peak with a maximum at 1203 K:** also observed for the $SrCO_3$ alone, assigned to its phase transformation from orthorhombic to hexagonal structure. The interfacial reaction between $SrCO_3$ and Al_2O_3 and

the formation of $SrAl_2O_4$ at temperatures below that of $SrCO_3$ phase transformation (~1203 K) requires activation energy of 130 kJ/mol for the carbonate decomposition [7]. At temperatures >1203 K, the crystallization of $SrAl_2O_4$ is dominated by diffusion of Al^{3+} ions into the $SrCO_3$ lattice co-existent with free SrO, and the activation energy for the carbonate decomposition decreases.

- **Endothermic peak with a maximum at 1323 K**: attributed to thermal decomposition of $SrCO_3$ with the release of —CO_2 (g), thus occurring about 100ºC below and being less deep in comparison to the single $SrCO_3$ component. This suggest the occurrence of a concomitant exothermic reaction due to the formation of strontium aluminates, in such a way that the heat released is consumed in the thermal decomposition of $SrCO_3$.
- **A broad exothermic band with a maximum at 1365 K:** due to the formation of crystalline strontium aluminates.
- **Endothermic peak with a maximum at 1485 K:** due to the second decomposition step of $SrCO_3$. The maximum weight loss is observed at about 1500 K.

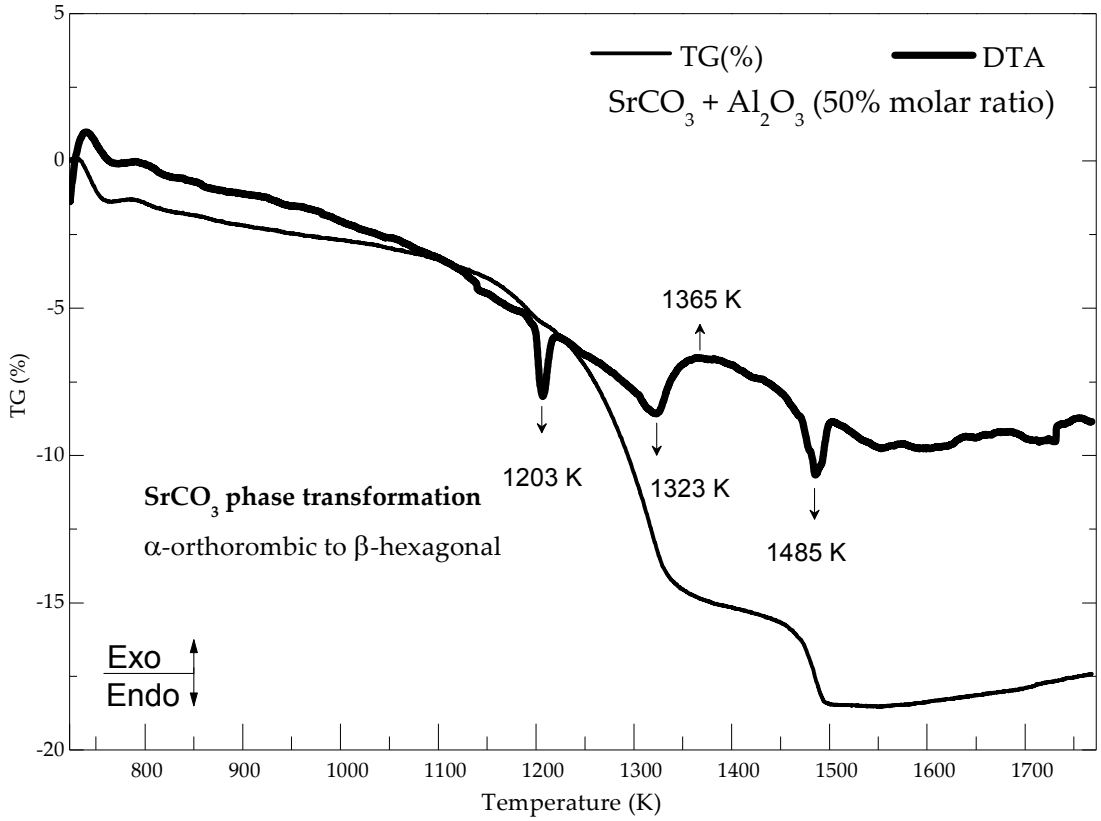

Figure 5. DTA and TG in *Argon* atmosphere at temperatures still 1773 K. b) thermogram of $SrCO_3$—Al_2O_3 (50% molar ratio).

According *Chang-Hsiang* [9b], the activation energy for $SrCO_3$ decomposition is significantly influenced by the calcination temperature, while the nature of alumina precursor, i.e. α-Al_2O_3 or γ-Al_2O_3, presents a secondary factor. The α-alumina used in this work might be obtained, for instance, from gibbsite ($\rightarrow \chi$-$Al_2O_3 \rightarrow \kappa$-$Al_2O_3 \rightarrow \alpha$-$Al_2O_3$) or boehmite ($\rightarrow \gamma$-$Al_2O_3 \rightarrow \delta$-$Al_2O_3 \rightarrow \theta$-$Al_2O_3 \rightarrow \alpha$-$Al_2O_3$) routes. The very shallow thermal effects observed with further increasing temperature suggest that the progresses towards the formation of more stable strontium aluminates are slow, as expected from diffusion controlled synthesis reactions. The theoretical enthalpies for the formation of $SrAl_2O_4$ host lattice are given by Eq. (4) to (8).

$$\Delta_r H^o(T_o) = \sum_i \nu_i \, \Delta_f H_i^o(T_o) \tag{4}$$

$$\Delta_r S^o(T_o) = \sum_i \nu_i \, S_i^o(T_o) \tag{5}$$

$$\Delta_r H^o(T) = \Delta_r H^o(T_o) + \int_{T_o}^{T} \sum_i \nu_i \, Cp_i(T)\, dT \tag{6}$$

$$\Delta_r S^o(T) = \Delta_r S^o(T_o) + \int_{T_o}^{T} \sum_i \nu_i \, \frac{Cp_i(T)}{T}\, dT \tag{7}$$

$$\Delta_r G^o(T) = \Delta_r H^o(T) - T\Delta_r S^o(T) \tag{8}$$

Where:
$\Delta_r H^o$ (T) = standard enthalpy change;
$\Delta_r S^o$ (T) = standard entropy change;
$\Delta_r G^o$ (T) = standard Gibbs energy change;
ν_i = stoichiometric coefficient of the compound;
C_p = heat capacity at constant pressure;
T = absolute temperature;
for initial (i) reactants or final (f) products.

The enthalpies of $SrCO_3$—Al_2O_3 reactions were studied from room temperature to about 1503 K (Fig. 6). The enthalpy changes confirmed that solid-state synthesis is favoured over 1300 K leading to the formation of better defined single phases from a direct reaction between SrO and Al_2O_3 (Eq. 3). The enthalpy of the solid-state synthesis attends the Hess Law, which states that the enthalpy change is independent of the route by which the reaction is achieved. The thermodynamic approach depends only on the initial and final stages of enthalpies. Standard enthalpy values ($\Delta_r H^o$ (T)) are positive for the Eq. (1) and (2) as endothermic reactions, and negative for Eq. (3) as an exothermic reaction, according the standards enthalpies reported elsewhere by [15], [16] and [18]. Thermodynamic equilibrium is obtained decreasing the enthalpy of the SrO, in accordance with the Eq. from (9) to (10).

$$\Delta_r G\,(T) = -RT \ln \frac{K\,(T)}{Q(T,P,\xi)} = \Delta_r G^o\,(T) + RT \ln Q(T,P,\xi) \tag{9}$$

$$\Delta_r G\,(T) = \Delta_r G^o\,(T) + RT \ln \prod_i a_i^{\nu i} \tag{10}$$

$$\Delta_r G\,(T) = \Delta_r G^o\,(T) + RT \ln \frac{P_{CO2}}{P^o} \tag{11}$$

Where:
R = gas constant;
T = absolute temperature;
K = equilibrium constant;
Q = heat transfer.
P = pressure;
ξ = degree of the advancement of the reaction;
$\Delta_r G^o$ (T) = standard Gibbs energy change;
Π_i = chemical potential in the standard state of the component i;
a_i = activity of the compound;
ν_i = stoichiometric coefficient of the compound.

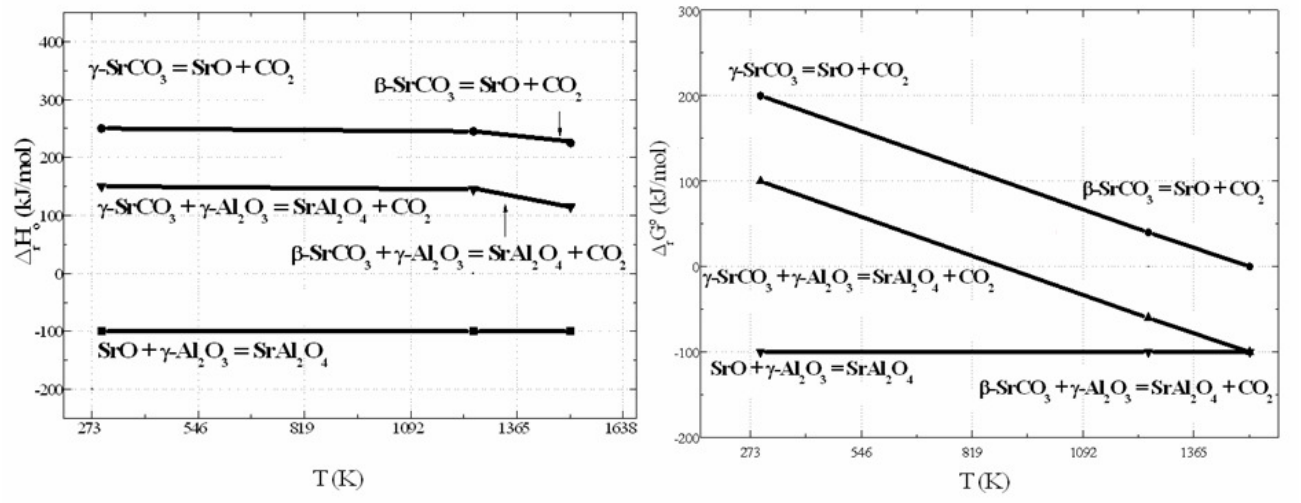

Figure 6. Thermodynamic properties of the $SrCO_3$—Al_2O_3 reactions from room temperature to about 1503 K: a) changes of the enthalpies; b) standard molar of free enthalpies [16, 18]. Data converted in Kelvin temperature.

3.2. Crystalline phases

Theoretical reactivity of reagents to obtain Sr aluminates by stoiquiometric solid state reaction among the constituents indicates that the activity degree of $(SrO).(Al_2O_3)$ and primary Al_4Sr arrangements are superior at 1473 than at 1573 K. Increasing the thermal energy, the activity of O_3Al_2-Al_2O_3 also is highest. Atoms in position of Al1 and Al4 are isoactives at 1473-1573 K, and in position of Al2 and Al3 have higher activity degrees at 1573 K. The activities of Sr-free ions are higher at 1573 K. Analogously, a catalyst boron-doped with B^{3+} ions on the Al^{3+} substitutional system are enabled to produces an activity degree to form tetrahedral BO_4 in the AlO_4 framework preferentially at 1573 K, upon the higher ionic activity of Al^{3+} free ions. At 1473 K, B^{3+} ions have a tendency to form B_4Sr, before the formation of the BO_4 tethahedra.

Boron doping replacing Al^{3+} ions generates distortions in the Al-framework and reduces the temperature required for the formation of the crystalline phases [19]. In these boric acid containing systems, the decomposition into B_2O_3 occurs in a first stage with the release of constitutional water at temperatures below 673 K, according to Eq. (11).

$$2\ H_3BO_{3\ (s)} \xrightarrow{\Delta} B_2O_3\ (s) + 3\ H_2O_{\ (g)} \quad (11)$$

Experimentally, the XRD patterns reveal that $SrAl_2O_4$ was formed, in conjunction with $Sr_3Al_2O_6$, upon holding the sample for 3 h at 1473 K in free (Fig. 7a) and pressed (Fig. 7b) powders. An increase of the intensity of $Sr_3Al_2O_6$ peaks was evidenced for the sample containing the highest amount of boron, and under the thermal treatment of recrystallization for 10 h (Fig. 7b). At the second stage of chemical interaction, there was the occurrence of mixed borate melt with intermediate compounds, which enhanced the diffusion phenomena thus, leading to an overall acceleration of the formation process of $SrAl_2O_4$, $Sr_3Al_2O_6$ and $Sr_3B_2O_6$, as described in Eq. from (12) to (15).

$$2\ SrCO_{3\ (s)} + SrAl_2O_{4\ (s)} \xrightarrow{\Delta} Sr_3Al_2O_{6\ (s)} + 2\ CO_{2\ (g)} \quad (12)$$

$$3\ SrCO_{3\ (s)} + Al_2O_{3\ (s)} \xrightarrow{\Delta} Sr_3Al_2O_{6\ (s)} + 3\ CO_{2\ (g)} \quad (13)$$

$$3\ SrCO_{3\ (s)} + B_2O_{3\ (s)} \xrightarrow{\Delta} Sr_3B_2O_{6\ (s)} + 3\ CO_{2\ (g)} \quad (14)$$

$$Sr_3Al_2O_{6\ (s)} + 2\ Al_2O_{3\ (s)} \xrightarrow{\Delta} 3\ SrAl_2O_{4\ (s)} \quad (15)$$

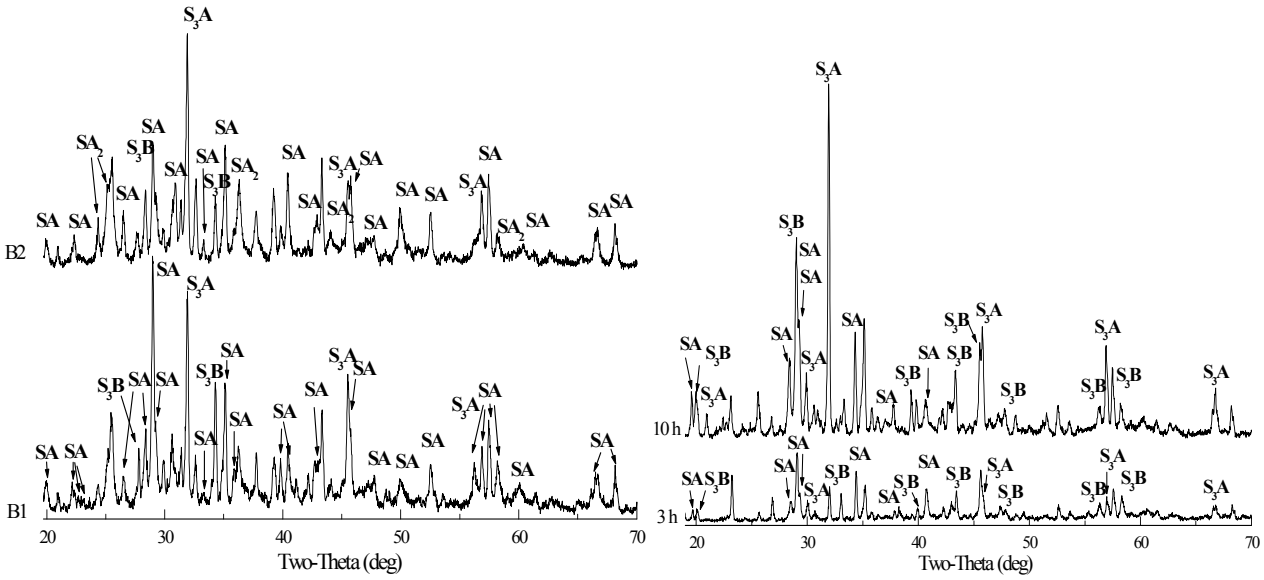

Figure 7. Effect of boron addition on X-ray diffraction profiles of samples annealed at 1473 K: a) B1 and B2 for 3 h, $SrAl_2O_4$ (SA), $SrAl_4O_7$ (SA_2), $Sr_3Al_2O_6$ (S_3A), and $Sr_3B_2O_6$ (S_3B); and b) B1 for 3 and 10 h, $SrAl_2O_4$ (SA), $Sr_3Al_2O_6$ (S_3A), and $Sr_3B_2O_6$ (S_3B).

In boron containing samples, the strontianite can be involved in cyclic borate reactions forming $Sr_3Al_2O_6$ and $SrAl_2O_4$ as major phases in successive reactions that might occur during the formation of these phases as described in Eq. (16) to (19). Note that when the boron oxide is reacting, intermediary strontium borates are formed.

$$Sr_3Al_2O_{6\ (s)} + 2\ B_2O_{3\ (s)} \xrightarrow{\Delta} SrAl_2O_{4\ (s)} + 2\ SrB_2O_{4\ (s)} \quad (16)$$

$$Sr_3B_2O_{6\ (s)} + Al_2O_{3\ (s)} \xrightarrow{\Delta} Sr_3Al_2O_{6\ (s)} + B_2O_{3\ (s)} \quad (17)$$

$$5\ SrCO_{3\ (s)} + 4\ Al_2O_{3\ (s)} \xrightarrow{\Delta} SrAl_2O_{4\ (s)} + Sr_3Al_2O_{6\ (s)} + SrAl_4O_{7\ (s)} + CO_{2\ (g)} \quad (18)$$

$$SrAl_4O_{7\ (s)} + SrB_2O_{4\ (s)} \xrightarrow{\Delta} 2\ SrAl_2O_{4\ (s)} + B_2O_{3\ (s)} \quad (19)$$

3.3. Nanostructure of strontium compounds

TEM image of the micro and nano-particles ($SrAl_2O_4$, $Sr_3Al_2O_6$ and $Sr_3B_2O_6$) obtained by increasing the annealing time to 10 h are showed in Fig. 8. The respective SAED pattern (Fig. 8b) of the region indicated in Fig. 8c reveals a nanostructure with spacing parameters of about 0.5 x 0.8 nm. This result is a possible $SrAl_2O_4$ detection, in agreement with the unit-cell parameters of the monoclinic structure (a=5.1607, b=8.822, c=8.4424, β=93.415, space group $P2_1$). EDX analysis comprised the boron atoms doping the structure replacing Al^{3+} sites (Fig. 8d).

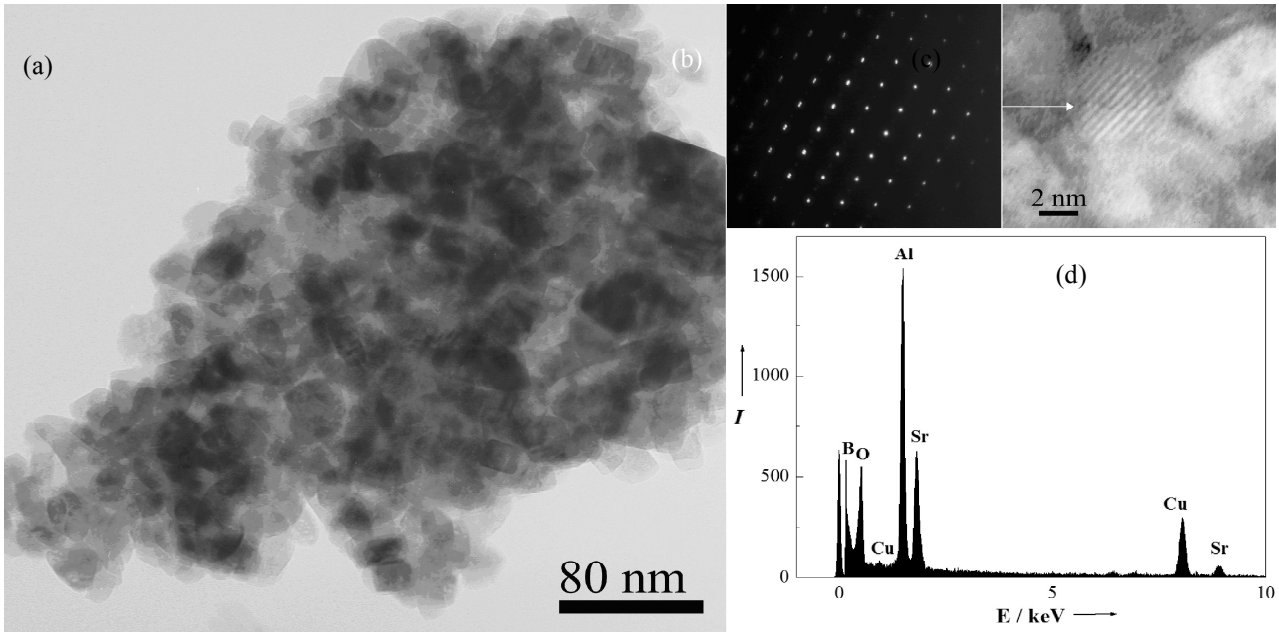

Figure 8. a) TEM of crystalline host lattice sample ($SrAl_2O_4$, $Sr_3Al_2O_6$, and $Sr_3B_2O_6$) obtained by pressing at 200 MPa and annealing at 1573 K for 10 h, and the respective b) SAED pattern of the c) indicated region; d) EDX analysis revealing boron atoms doping the crystal structure.

4. CONCLUSION

In the phosphor industry, the solid-state synthesis carried out within the temperature range of 1473-1573 K using a catalyst boron-doping revealed to be an effective route to prepare large-scale micro- and nano- particles of Sr-aluminates nano phosphors.

5. ACKNOWLEDGEMENTS

This work was supported by the Ministry of Science, Technology and Higher Education (MCTES) and Research Institute of University of Aveiro (PT).

6. REFERENCES

[1]. Afterglow phenomenon, see: a) J. KAPLAN, A New Afterglow Phenomenon, *Phys. Rev*. **1940**, *57*, 662-662; b) H. G. JENKINS, J. N. BOWTELL, R. W. STRONG, Afterglow Phenomena in Argon-Nitrogen Mixtures at Pressures Close to Atmospheric, *Nature*, **1949**, *163*, 401-402, DOI:10.1038/163401a0; c) *Astronomy & Astrophysics*, **2001**, *379*, L39-L43; d) R. SAGAR, Another Indian optical observation of a gamma-ray burst afterglow from UPSO, *Current Science*, **2000**, *78*, 5; e) C. C. KANG, R. S. LIU, J. C. CHANG, B. J. LEE, Synthesis and Luminescent Properties of a New Yellowish-Orange Afterglow Phosphor Y_2O_2S:Ti, Mg, *Chem. Mater*. **2003**, *15*, 3966-3968; f) S. SHIONOYA, W. M. YEN, Phosphor Handbook, *CRC Press*, **1998**.

[2]. a) T. MATSUZAWA, Y. AOKI, N. TAKEUCHI, Y. MURAYAMA, A new long phosphorescent phosphor with high brightness $SrAl_2O_4$:Eu^{2+}, Dy^{3+}, *J. Electrochem. Soc.* **1996**, *143*, 2670–2673; b) Y. H. LIN, Z. T. ZHANG, F. ZHANG, Z. L. TANG, Q. Y. CHEN, Preparation of the ultrafine $SrAl_2O_4$:Eu, Dy needle-like phosphor and its optical properties, *Mater. Chem. Phys*. **2000**, *65*, 103.

[3]. a) T. AITASALO, P. DEREN, J. HÖLSA, H. JUNGNER, J. C. KRUPA, M. LASTUSAARI, J. LEGENDZIEWICZ, J. NIITTYKOSKI, W. STREK, Persistent luminescence phenomena in materials doped with rare earth ions, *J. Solid-state Chem*. **2003**, *171*, 114–122; b) J. HÖLSA, H. JUNGNER, M. LASTUSAARI, J. NIITTYKOSKI, Persistent luminescence of Eu^{2+} doped alkaline earth aluminates MAl_2O_4: Eu^{2+}, *J. Alloys Comp.* **2003**, *354*, 326–330.

[4]. S. H. M. POORT, W. P. BLOKPOEL, G. BLASSE, Luminescence of Eu^{2+} in barium and strontium aluminate and gallate. *Chem. Mater*. **1995**, *7*, 1547-1551.

[5]. W. S. SHI, H. YAMADA, K. NISHIKUBO, H. KUSABA, C. N. XU, Novel structural behavior of strontium aluminate doped with europium, *J. Electrochem. Soc*., **2004,** *151*, 5, H97-100.

[6]. Z. FU, S. ZHOU, S. ZHANG, Study on optical properties of rare-earth ions in nanocrystalline monoclinic $SrAl_2O_4$: Ln (Ln= Ce^{3+}, Pr^{3+}, Tb^{3+}), *J. Phys. Chem. B* **2005**, *109*, 14396–14400.

[7]. A. DOUY, M. CAPRON, Crystallisation of spray-dried amorphous precursors in the $SrO–Al_2O_3$ system: a DSC study, *J. Eur. Ceram. Soc.* **2003**, *23*, 2075–2081.

[8]. B. N. OKERIYA, D. S. TSAGARESHVILI, G. G. GVELESYANI, Enthalpy and heat capacity of strontium aluminate at high temperatures, *F. Techn. Div. AFB Ohio,* **1972**.

[9]. a) A. M. ABAKUMOV, O. I. LEBEDEV, L. NISTOR, G.VAN TENDELOO, S. AMELINCK, The ferroelectric phase transition in tridymite type $BaAl_2O_4$ studied by Electron Microscopy, *Phase Trans*., **2000**, *71*, 2, 143–160; b) Y. L. CHANG, H. I. HSIANG, Phase evolution during formation of $SrAl_2O_4$ from $SrCO_3$ and α-Al_2O_3/AlOOH, *J. Am. Ceram. Soc*., **2007**, *90*, 9, 2759–2765.

[10]. N.K. ZURBA, Persistent luminescence of $SrAl_2O_4$:Ce(III), Dy, Eu nanotubes, nanowires and core-shells for people with disabilities: nano-emergency, Doctoral Thesis, *University of Aveiro*, **2010**, 168p.

[11]. Aluminates: a) K. R. S. PREETHI, C. H. LU, J. THIRUMALAI, R. JAGANNATHAN, T. S. NATARAJAN, N. U. NAYAK, I. RADHAKRISHNA, M. JAYACHANDRAN, D. C. TRIVEDI, $SrAl_4O_7$:Eu^{2+} nanocrystals: synthesis and fluorescence properties, *J. Phys. D: Appl. Phys.* **2004**, *37*, 2664-2669; b) A. NAG, T. R. N. KUTTY, The mechanism of phosphorescence of $SrAl_{2-x}B_xO_4$ ($0<x<0.2$) and $Sr_4Al_{14-x}B_xO_{25}$ ($0.1<x<0.4$) co-doped with Eu^{2+} and Dy^{3+}, *Mat. Res. Bull.* **2004**, *39*, 331-342 ,c) S. H. HAN, Y. J. KIM, Luminescent properties of Ce and Eu doped $Sr_4Al_{14}O_{25}$ phosphors, *J. Opt. Mat.* **2005**, *28*, 6-7, 626-630; d) T. TAKEDA, K. TAKAHASHI, K. UHEDA, H. TAKIZAWA, T. ENDO, Crystal structure and luminescence properties of $Sr_2Al_6O_{11}$:Eu^{2+}, *J. Japan Soc. Powder Metal*. **2002**, *49*, 12, 1128-1133 ; e) J. S. CHOI, S. H. BAEK; S. G. KIM, S. H. LEE, H. L. PARK, S. I. MHO, T. W. KIM, Y. H. HWANG, Energy transfer between Ce^{3+} and Eu^{2+} in $SrAl_{12}O_{19}$:Ce_x^{3+}, $Eu_{0.01}^{2+}$ (x= 0.01-0-09), *Mat. Res. Bull.* **1999**, *34*, 4, 551-556; f) C. YUESHENG, Z. PING, Z. ZHENTAI, Eu^{2+} and Dy^{3+} co-doped $Sr_3Al_2O_6$ red long-afterglow phosphors with new flower-like morphology, *J. Phys. B: Phys. Cond. Matt*. **2008**, *403*, 21-22, 4120-4122; g) R. W. HYLAND JR, J. P. QUINTENZ, B. T. DUNVILLE, G. SUBRAHMANYAM, Photoluminescent Alkaline Earth Aluminate and Method for Making the Same, *US6969475 Appl. Pat*. **2005**, *11*, 29; h) C. ZHAO, D. CHEN, Y. YUAN, M. WU, Synthesis of $Sr_4Al_{14}O_{25}$:Eu^{2+}, Dy^{3+} phosphor nanometer powders by combustion processes and its optical properties, *Mater. Science Eng. B* **2006**, *133*, 1-3, 200-204.

[12]. L. WANG, Y. ZHU, Preparation of nano-sized $SrAl_2O_4$ using an amorphous hetero-nucleus complex as a precursor, *J. Alloys Comp.,* **2004**, *370*, 276–280.

[13]. M. L. RUIZ-GONZÁLEZ, J. M. GONZÁLEZ-CALBET, M. VALLET-REGI, E. CORDONCILLO, P. ESCRIBANO, J. B. CARDA, M. MARCHAL, Planar defects in a precursor for phosphor materials: $SrAl_{2-x}B_xO_4$ ($x < 0.2$), *J. Mater. Chem*., **2002**, *12*, 1128–1131.

[14]. F. MASSAZZA, Diagram phase of SrO—Al_2O_3 system, *La chimica e l´industria* – XLI, **1959**, *2*, 108-115.

[15]. O. KNACKE, O. KUBASCHEWSKI, K. HESSELMANN, Thermochemical Properties of Inorganic Substances, *Springer Verlag*, 2nd, **1991**, I-II.

[16]. J. J. LANDER, Polymorphism and anion rotational disorder in the alkaline earth carbonates, *J. Chem. Phys*., **1949**,*17*, 892–0.

[17]. P. ESCRIBANO, M. MARCHAL, M. L. SANJUÁN, P. A. GUTIÉRREZ, B. JULIÁN, E. CORDONCILLO, Low-temperature synthesis of $SrAl_2O_4$ by a modified sol–gel route: XRD and Raman characterization, *J. Solid-state Chem.* **2005**, *178*, 6, 1978–1987.

[18]. C. BEAUGER, Elaboration, Characterisation et Modelisation des Phenomenes de Luminescence du Monoaluminate de Strontium Dope a l´Europium et au Dysprosium $SrAl_2O_4$:Eu, Dy, Doctoral Thesis, *Inst. Nat. Polyt. Grenoble,* **1999**, 47-87.

[19]. A. NAG, T. R. N. KUTTY, Role of B_2O_3 on the phase stability and long phosphorescence of $SrAl_2O_4$: Eu, Dy, *J. Alloys Comp.,* **2003**, *354*, 221–231.